



Optimizing fatty acids composition in meat-like tissue derived from myogenic conversion of pig fibroblasts



Pengxiang Zhao^{1,3}, Jianqi Lv^{1,3}, Wei Gu², Hao Mi², Haiying Cui², Lei Chen², Alexander Kurdeko² & Heng Wang¹✉

Fibroblasts are abundant throughout the body and easily accessible without animal sacrifice. They possess the ability to proliferate and differentiate into muscle and fat tissues, as well as to produce extracellular matrix components, making them ideal for cultured meat production. In this study, we utilized the pig fibroblasts as seed cells and conducted myogenic/lipogenic transdifferentiation in 3D to create a muscle/fat matrix constituting whole-cut meat within 9 days. The muscle cells were efficiently derived from the fibroblasts overexpressing *MyoD* and the subsequent lipid deposition into the muscle was achieved by supplementing with a lipogenic inducer composed of olive oil and soybean lecithin. Lipidomic analysis revealed that the engineered meat exhibited a healthier fatty acid profile compare to conventional pork, with reduced saturated fatty acids (44.49% vs. 51.2%) and increased polyunsaturated fatty acids (31.33% vs. 27.01%). These findings open new avenues for customized cultured meat production with optimized fatty acids compositions tailored to meet the diverse consumer demands.

Cultured meat has been proposed as a viable alternative to enhance global food security and sustainability, by significantly reducing land, water use, and greenhouse gas emissions^{1,2}. This innovative approach involves extracting a small number of cells from healthy animals and cultivating them in a sterile environment with specific culture media, with the goal of generating tissues that approximate the cellular and structural features of traditional meat³. Cultured meat is often proposed to offer benefits such as reduced environmental impact, improved food safety^{4,5}, customizable nutritional and sensory properties^{6,7}. However, these advantages are still largely theoretical^{8,9}. Their technical, economic, and regulatory feasibility remains the subject of ongoing debate^{10,11}. Current research on cultured meat mainly focuses on the differentiation of muscle and fat by utilizing multipotent stem cells or specialized somatic cells^{12–14}. However, employing stem cells as the primary source for cultured meat presents considerable challenges. Their limited proliferation and differentiation capacities, coupled with their relative scarcity in animals, make them difficult to obtain and cultivate, hindering large-scale production¹⁵.

Fibroblasts are a promising cell source for cultured meat production due to their abundance, ease of isolation, and capacity for myogenic and adipogenic transdifferentiation^{16–18}. It has been reported that fibroblasts can be used as source cells for cultured meat production^{19,20}. Our previous

research demonstrated that overexpressing Myogenic differentiation (*MyoD*) in fibroblasts from pigs, chickens, and mice can induce their conversion into muscle cells²¹. *MyoD* is a key muscle regulatory factor (MRF) expressed in early muscle lineage cells, as well as myogenin (*MyoG*), myogenic factor 5 (*Myf5*) and myogenic factor 6 (*Myf6*)²². *MyoD* acts as a master regulator and, together with *Myf5* and *Myf6*^{23–25}, induces *MyoG* expression for terminal muscle differentiation^{26,27}. Notably, we have successfully used chicken fibroblasts for transdifferentiation, enabling controlled deposition of intramuscular fat in mixed muscle-fat cultured meat²⁸. These findings highlight the potential of fibroblasts as seed cells for sustainable cultured meat production.

Beyond muscle formation, fat deposition is equally critical for cultured meat quality. Intramuscular fat contributes to improved meat quality, flavor and consumer acceptance^{29,30}. More importantly, the balance between saturated and unsaturated fatty acids affects human health, with excess saturated fats damaging health and unsaturated fats such as oleic and linoleic acids being metabolically beneficial³¹. Traditional adipogenic inducers, such as insulin, rosiglitazone raises concerns regarding food safety and regulatory approval^{32–34}. Therefore, there is a growing need for natural, food-grade alternatives that promote lipid accumulation while maintaining cellular viability. Natural alternatives such as olive oil (rich in

¹College of Animal Science, Shandong Provincial Key laboratory for Livestock Germplasm Innovation & Utilization, Shandong Agricultural University, Taian, China.

²Shandong Provincial Key Laboratory of Animal Microecology and Efficient Breeding of Livestock and Poultry, Baolai-Leelai Bio-Tech, Taian, China. ³These authors contributed equally: Pengxiang Zhao, Jianqi Lv. ✉e-mail: wangheng@sdau.edu.cn

monounsaturated fatty acids) offer a safer way to both promote lipid accumulation and improve the fatty acid composition of cultured meat³⁵.

To address the limitations of stem cell-based cultured meat, this study aimed to establish a fibroblast-based 3D culture system that supports both muscle and fat tissue formation. We hypothesized that porcine fibroblasts could transdifferentiate into muscle and fat in a three-dimensional environment. Moreover, a food-grade adipogenic inducer consisting of olive oil and soy lecithin promotes fat deposition and improves the fatty acid composition of the produced pig muscle tissues. To test this hypothesis, we used a GelMA hydrogel to culture porcine fibroblasts, induced muscle differentiation through transient *MyoD* overexpression, and applied our lipogenic inducer to stimulate lipid accumulation. The results showed an efficient combination of muscle and fat and enrichment in unsaturated fatty acids, suggesting a healthier meat composition and nutritional value compared to conventional pork. This finding demonstrated that fibroblast-derived cultured meat could achieve a favorable fatty acid composition, with higher levels of unsaturated fatty acids, offering a healthier and more sustainable alternative to traditional meat products.

Results

3D culture of porcine fibroblasts in hydrogels

In our previous work, we developed a GelMA hydrogel model for 3D cell culture and successfully proliferated and differentiated chicken fibroblasts within this matrix. Building on this, we now explore the use of a similar 3D scaffold for culturing porcine fibroblasts. We cultured porcine fibroblasts in growth medium containing 15% FBS and monitored the growth of cells seeded in GelMA hydrogel at multiple time points: 1 hour, 1 day, 3 days, 5 days, 7 days, and 9 days. At 1 h post-seeding, the cells appeared spherical, typical of the initial stage of culture. By 1 day, the cells began extending outward, and by day 5, they had developed into a multi-“tentacle” shape. By day 9, the cells had formed an extensive, dense network, indicating active proliferation within the hydrogel matrix. (Fig. 1A). To assess the proliferation capacity, we performed an EdU assay on fibroblasts at different

time points. The results showed a gradual increase in proliferation capacity over time (Fig. 1B, C). This demonstrated that porcine fibroblasts not only maintained their normal physiological characteristics but also exhibit robust proliferation in the hydrogel matrix.

Myogenic transdifferentiation of porcine fibroblasts in 3D

The fibroblasts can transdifferentiate into muscle cells via the ectopic expression of skeletal muscle lineage transcription factor *MyoD*. To achieve the myogenic transdifferentiation of porcine fibroblasts while avoiding the safety concerns associated with genetically modified food, we utilized the adenoviral transient *MyoD* overexpression without the genomic integration (Figure S1). Myosin heavy chain 1 (MHC) immunofluorescence staining showed that differentiation capacity increased with *MyoD* overexpression (Figure S2). Subsequently, we compared the effects of myogenesis induced by two culture media, 15% FBS and 2% horse serum (HS). Initial 2D culture optimization showed that differentiation in 2% HS led to higher MHC expression and multinucleated myotube formation compared to 15% FBS, which produced only limited muscle markers and irregular cell morphology (Figure S3). Therefore, 2% HS was selected for subsequent 3D myogenic differentiation.

For efficient large-scale cultured meat production, cells were first seeded in the GelMA hydrogel until reaching appropriate cell density. Then, *MyoD* adenovirus were infected cells and induced myogenic transdifferentiation. However, viral diffusion within the hydrogel was limited, which reduced infection efficiency. To enhance this, we incorporated polyethylene oxide (PEO) as a porogen³⁶, forming a sponge-like porous hydrogel that enhances diffusion and improves adenovirus infection efficiency (Figure S4).

Next, we conducted myogenic transdifferentiation of porcine fibroblasts in 3D (Fig. 2A). The cells were first seeded in hydrogel for proliferation for 2 days. Upon *MyoD* overexpression and the induced myogenic differentiation, we observed abundant muscle formation, as evidenced by the formation of densely packed MHC+ myotubes (Figs. 2C, D, Supplementary

Fig. 1 | 3D culture of porcine fibroblasts in hydrogel matrix. **A** Bright field observations of porcine fibroblasts grew in GelMA hydrogel at 1 hour, 1 day, 3 days, 5 days, 7 days, and 9 days. Scale bar, 50 μ m. **B** Representative images of EdU staining of porcine fibroblasts in GelMA hydrogel at 1 day, 5 days, and 9 days. Scale bar, 50 μ m. **C** Quantification of the proportion of EdU-positive proliferating cells in (B). Error bar = mean \pm SD ($n = 3$ independent cultures per time point). Statistical analysis was performed using one-way ANOVA. Post hoc multiple comparisons were conducted using Tukey’s test to identify significant differences between time points.

*** $p < 0.001$. * $p < 0.05$.

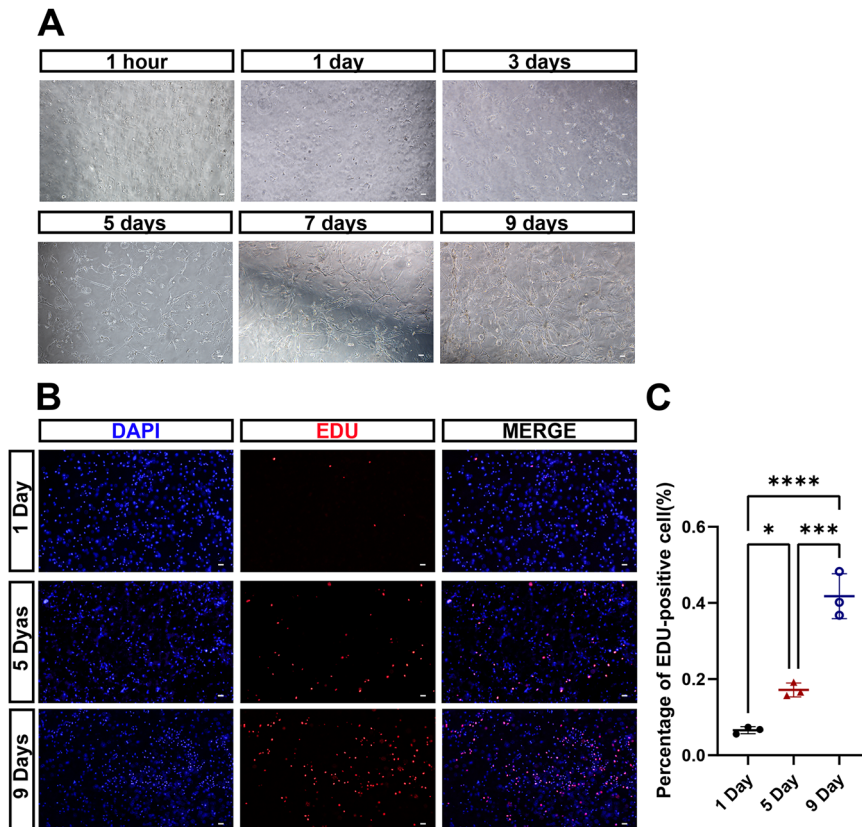
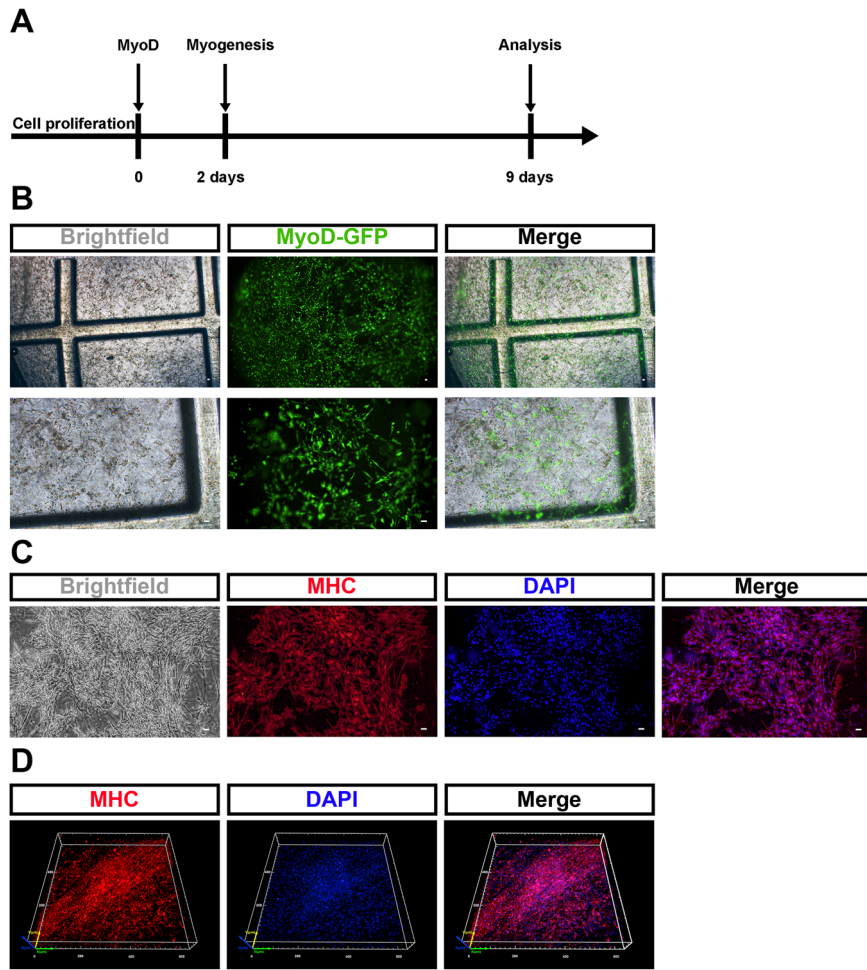


Fig. 2 | Myogenic transdifferentiation of porcine fibroblasts in 3D. A Experimental design for myogenic transdifferentiation of fibroblasts into muscle cells in 3D culture. B Representative live fluorescence images showing the MyoD-GFP expression in porcine fibroblasts in 3D culture. Scale bar, 50 μ m. C Representative immunostaining images of myosin heavy chain 1 (MHC) staining showing the myogenic transdifferentiation of porcine fibroblasts in 3D culture. Scale bar, 50 μ m. D 3D images of MHC immunostaining of transdifferentiated muscle cells in 3D culture.



video1). Therefore, we successfully produced skeletal muscle 3D cell model via the myogenic transdifferentiation of porcine fibroblasts.

Induction of lipid droplet formation in porcine fibroblasts in 3D
 Fat content plays a crucial role in the meat flavor, texture, and nutritional value. Since fibroblasts have intrinsic adipogenesis potential, we intended to induce cellular lipid accumulation in 3D culture system. To achieve this, we developed a food-derived lipogenic inducer composed of olive oil and soybean lecithin, both rich in unsaturated fatty acids. Oil Red O staining confirmed the presence of red, spherical lipid droplets (LDs) in the emulsified mixture (Figure S5A and B). The laser nanoparticle sizer analysis showed that the particle sizes were mainly concentrated around 100 ± 50 nm (Figure S5C), ensuring efficient diffusion into the hydrogel.

To determine the optimal concentration, porcine fibroblasts were treated with increasing doses of the lipogenic inducer in 2D culture. Oil Red O staining showed a dose-dependent increase in cellular LDs accumulation, with the highest concentration of 16,000 μ g/mL (Fig. 3A). This concentration was then applied to 3D cultures, where cells successfully accumulated LDs after two days of induction (Fig. 3B). Oil Red O staining revealed the red, bead-like LDs distributed throughout the entire cell (Fig. 3C). Hence, the porcine fibroblasts could be efficiently induced to deposit fat in 3D conditions.

Preparation of muscle and fat mixed cultured meat

After confirming the optimal conditions for the formation of muscle and fat, respectively, we combined these processes to generate structured muscle-fat cultured meat products from a single fibroblast source. First, porcine fibroblasts were transdifferentiated into muscle cells through overexpressed *MyoD* in 3D hydrogel. Once myogenesis was established, the olive oil-based

lipogenic inducer was introduced to promote lipid deposition, simulating intramuscular fat formation (Fig. 4A).

Immunostaining confirmed the presence of abundant MHC-positive myotubes, while the bright field observation and Oil Red O staining revealed intracellular LDs, indicating successful co-induction of muscle and fat (Fig. 4B). The Live/Dead staining results (Calcein-AM and PI) clearly showed that cells remained highly viable under all conditions, as indicated by widespread green fluorescence and minimal PI-positive (dead) cells (Fig. 4C). This indicates that the cells were actively proliferating and integrating within the 3D hydrogel scaffold. RT-qPCR analysis revealed a significant upregulation of myogenic markers (*MyoD*, *MyoG*, *Myf5*, and *Myf6*) in the transdifferentiated cells (Fig. 4E). Additionally, the expression of two lipid metabolism-related genes (*DGAT1* and *DGAT2*) was also elevated, suggesting endogenous triglyceride synthesis within the cells (Fig. 4D).

Western blot analysis demonstrated sustained expression of MYH1, even after lipid induction, indicating that adipogenesis did not interfere with myogenic transdifferentiation (Fig. 4F, G). The appearance of 3D cultured meat showed a red block-like structure, forming a product rich in muscle and fat. In contrast, the cell-free hydrogel matrix presented a transparent, soft blocky structure (Fig. 4H). To better identify the structural characteristics of GelMa scaffold under different cellular conditions, we performed Scanning Electron Microscopy (SEM) imaging. The GelMA scaffold displayed a highly porous and interconnected network structure with well-defined pore walls. At higher magnification (5 μ m), the pore surfaces appeared smooth and unoccupied, indicating the absence of cellular material. After myogenic differentiation, the scaffold exhibited a denser structure with fibrous material bridging across pores. At higher magnification, aligned, thread-like structures were visible, resembling early-stage myotube formation and extracellular matrix deposition, indicating

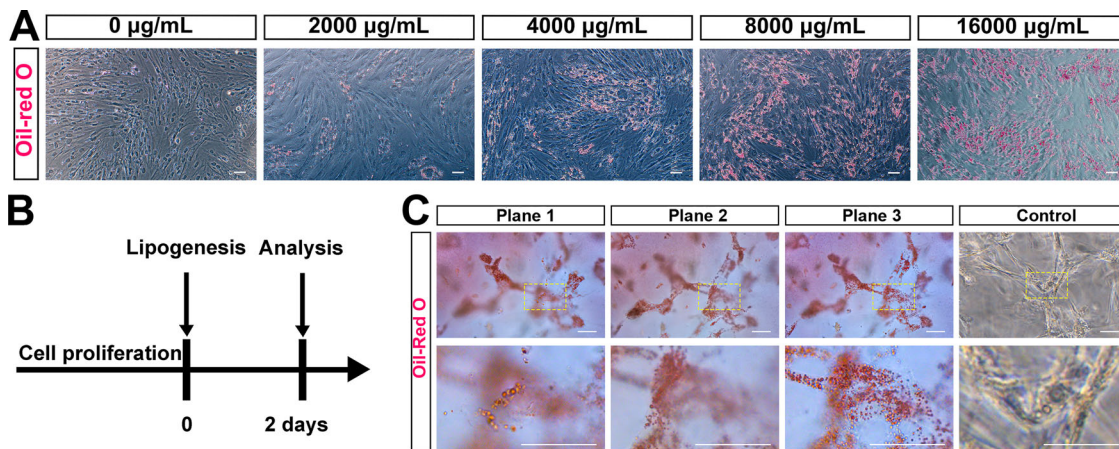


Fig. 3 | Induction of lipid droplet formation in porcine fibroblasts in 3D.

A Representative images showing Oil red O staining of porcine fibroblasts following induction with various concentrations of olive oil-based lipogenic inducers in 2D culture. The arrow indicates large lipid droplets. Scale bar, 50 μ m. B Experimental

design for lipid droplet formation in porcine fibroblasts in 3D. C Representative images showing Oil Red O staining of lipid droplet formation in cells in 3D culture at different focal planes at the same position. Scale bar, 50 μ m.

successful muscle tissue development. In the myogenesis and lipogenesis condition, the scaffold became more homogenized and densely packed. Rounded, lipid-like inclusions were visible, indicating successful adipogenic differentiation alongside muscle tissue formation (Fig. 4I).

Enrichment of unsaturated fatty acid in the cultured meat

Fatty acid composition is a key determinant of meat quality, influencing both its nutritional value and sensory attributes. In cultured meat, adjusting fatty acid profiles is essential for replicating the taste and texture of conventional meat while enhancing health benefits. To evaluate how our lipogenic induction strategy modified the lipid composition, we performed lipidomic analysis and compared the fatty acid profile of the cultured meat with conventional pork.

Cultured meat contained a lower proportion of saturated fatty acids (44.49%) compared to pork (51.20%), while monounsaturated fatty acids (24.18% vs. 21.79%) and polyunsaturated fatty acids (31.33% vs. 27.01%) were enriched (Fig. 5A). This transition to unsaturated fatty acids suggests that the lipid composition of cultured meat can be effectively regulated by adipogenesis inducers. Further analysis of the top 10 most abundant fatty acids showed that cultured meat had higher levels of oleic acid (FA 18:1), linoleic acid (FA 18:2), and α -linolenic acid (FA 18:3, ω -3), while myristic acid (FA 14:0) and stearic acid (FA 18:0) were reduced (Fig. 5B). Given that olive oil, a key component of the lipogenic inducer, is naturally rich in oleic and linoleic acids, its incorporation likely contributed to these compositional changes.

Despite the different proportions of individual fatty acids, the overall lipid composition of cultured meat was very similar to that of conventional pork. By comparing the top 10 most abundant fatty acids in pork and cultured meat, we found that 7 of them were common to both, accounting for 84.62% in pork and 87.27% in cultured meat (Fig. 5C, D). These results demonstrate that fatty acid composition in cultured meat can be precisely modulated through lipid supplementation strategies. By incorporating olive oil and soybean lecithin as natural adipogenic inducers, we successfully enhanced the proportion of health-promoting unsaturated fatty acids while reducing less desirable saturated fats. This approach not only improves the nutritional value of cultured meat but also provides a scalable strategy for tailoring fat composition to meet consumer preferences and dietary recommendations.

Discussion

Cultured meat has emerged as a promising alternative to traditional livestock-based meat, with potential benefits in terms of environmental conservation and health³⁷. Life cycle assessments suggest that cultured meat may significantly mitigate the environmental and public health burdens

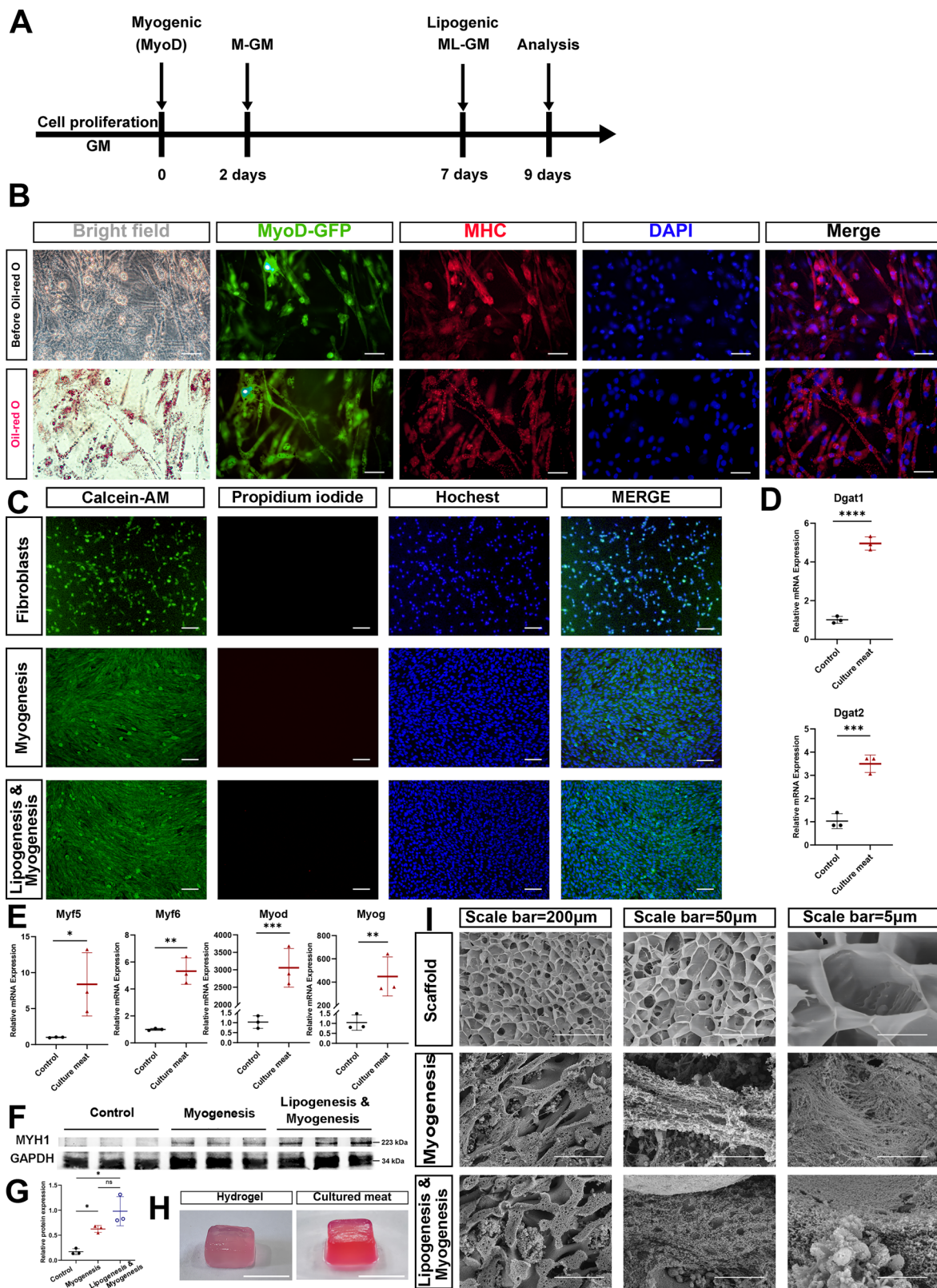
associated with traditional meat production³⁸. Our findings provide a new approach to cultured meat, contributing to its potential use as a functional, available food choice. By adjusting the fat content and fatty acid composition, we produced the meat that meets the demands of the modern diet, including a reduction in saturated fats while increasing unsaturated fats³⁹.

A key goal of this study was to improve the fatty acid profile of cultured meat. We used a natural, food-grade lipogenic inducer made from olive oil and soybean lecithin^{40,41}, which increased the proportion of beneficial unsaturated fatty acids, including oleic and linoleic acids. These changes reduce the saturated fat associated with metabolic disease^{42,43} and bring the fatty acid composition of cultured meat more consistent with heart-healthy dietary guidelines^{44,45}. The modified fatty acid composition allows cultivated meat to become a healthier alternative compared to conventional meats⁴⁶. Our studies also developed a natural lipogenic inducer consisting of olive oil and soy lecithin. This approach replaces chemical lipogenesis inducers (e.g., insulin or rosiglitazone) and provides a safer, more sustainable alternative⁴⁷. It avoids the long-term health effects and regulatory approval issues of chemical lipogenesis inducers. The use of natural, food-grade ingredients also enhances the potential for further applications of cultured meat.

This study highlights fibroblasts as an effective cell source for producing muscle-fat mixed cultured meat. Fibroblasts have several advantages over traditional stem cells. They are abundant, easy to isolate, and grow quickly. Their ability to transform into both muscle and fat cells helps create structured tissue from a single source. This simplifies production and improves scalability^{19,20}. Fibroblast-based cultured meat more closely resembles traditional meat in texture and composition, making it a strong candidate for large-scale production.

Despite these advancements, the study has some limitations. First, experiments were conducted on a small scale using 2D and 3D culture models. While these models show how cells differentiate and accumulate lipids, scaling up production remains a challenge. Future studies should develop bioreactor systems that allow large-scale production while maintaining meat quality and structure. Additionally, although higher PUFA content improves health value, it may compromise oxidative stability. Incorporating food-grade antioxidants in future formulations could help preserve quality and extend shelf life.

Another limitation of this study is the use of animal-derived serum in the culture medium, which raises both ethical and sustainability concerns. The reliance on serum is inconsistent with the broader goal of reducing dependence on animal products in cultured meat production. Although serum remains widely used in early-stage research to support cell proliferation and differentiation, future work should prioritize the development of serum-free media^{7,14,48}. Such advancements would not only enhance ethical acceptability and environmental sustainability but also improve consumer acceptance.



In conclusion, this study demonstrates the potential of fibroblasts for producing high-quality cultured meat with improved fatty acid composition. The use of natural lipogenic inducers and advanced 3D culture methods is a step toward healthier and more sustainable meat alternatives. Challenges remain, such as scaling up production and removing serum from the culture process. Nevertheless, our findings provide novel strategies for future advancements in customized cultured meat technology.

Materials and Methods

Preparation of MyoD overexpressing adenovirus

Construction of *MyoD* overexpression vector: The CMV-mouse *MyoD* fragment was excised from the modified shuttle plasmid (HedgehogBio, HH-CAS-056) using the EcoRI restriction enzyme (Yugong Bio, EG15536S). Two primers were designed, and the CMV-pig *MyoD* fragment was amplified using a plasmid containing the target pig *MyoD* sequence as

Fig. 4 | Preparation of muscle and fat mixed cultured meat. **A** Experimental design for porcine fibroblast myogenic and lipogenic differentiation in 3D culture. **B** Representative images of MHC and Oil Red O staining of cells upon myogenesis/lipogenesis in 3D culture. Scale bars, 50 μ m. **C** Fluorescence imaging of cell viability assay of three-dimensional GelMA constructs under differentiation conditions. Live/dead staining with calcein-AM (green, live cells) and propidium iodide (red, dead cells), with nuclei counterstained with Hoechst (blue). Scale bars, 50 μ m. **D, E** Expression of myogenic genes and lipogenic genes in the cells of cultured meat and 3D porcine fibroblasts without any stimulation(control) by RT-qPCR. Error bars indicate s.e.m ($n = 3$ independent cultures). * $P < 0.05$, ** $P < 0.01$, *** $P < 0.001$. **F** Western blotting showing the expression levels of MHC and GAPDH in porcine fibroblasts undifferentiation(control), myogenic differentiation, myogenic and lipogenic differentiation in 3D culture. $n = 3$. **G** Quantification of relative protein expression normalized to GAPDH. Band intensities were measured using ImageJ, and values represent the ratio of target protein to GAPDH from three independent experiments. Data are shown as mean \pm SD. Statistical significance was determined using one-way ANOVA. * $p < 0.05$ was considered significant. **H** Macroscopic morphology of the GelMA hydrogel scaffold(left) and cultured meat (right). Scale bars, 1 cm. **I** Microstructure of 3D GelMA constructs under different differentiation conditions by scanning electron microscopy. Scale bars, 100 μ m.

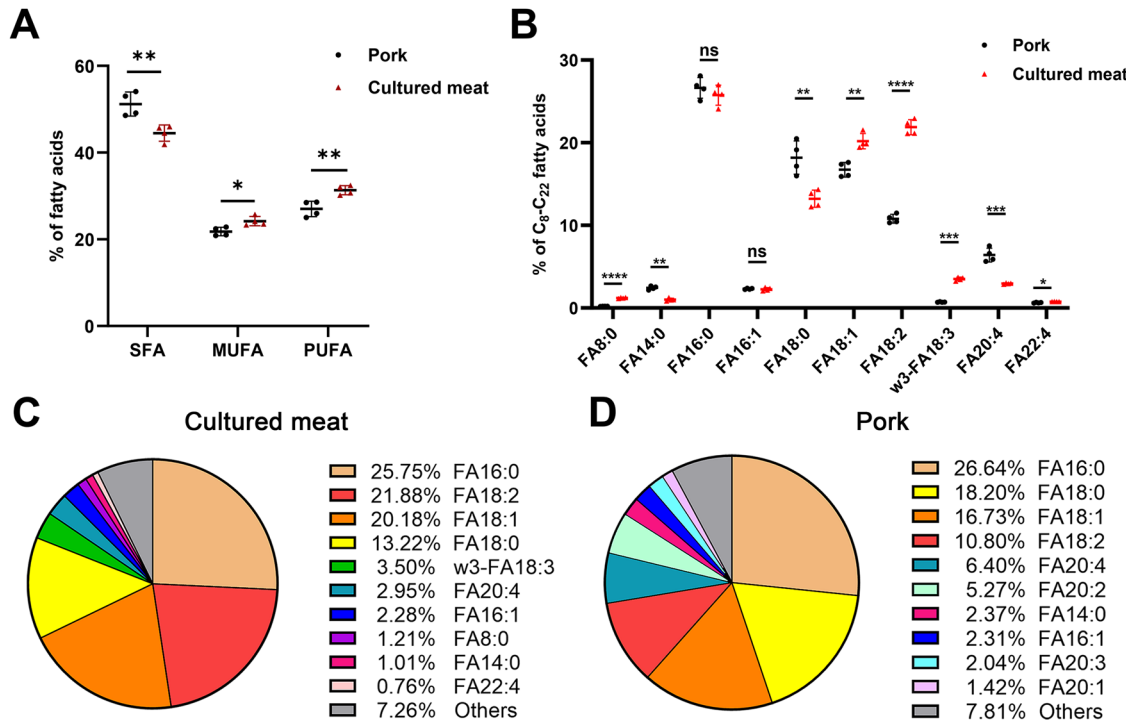


Fig. 5 | Unsatuated fatty acid enrichment in the cultured meat. **A** Proportion of C8-C22 fatty acids categorized by degree of saturation between pork and cultured meat. SFA: Saturated fatty acid. MUFA: monounsaturated fatty acid. PUFA: polyunsaturated fatty acid. Error bars indicate s.e.m, $n = 4$ of each group. * $P < 0.05$, ** $P < 0.01$. **B** Proportion of the top 10 fatty acids in cultured meat of C8-C22 fatty acids between pork and cultured meat. Error bars indicate s.e.m, $n = 4$ of each group. *** $P < 0.01$, *** $P < 0.001$, **** $P < 0.0001$, ns: not significant. **C, D** Detailed Proportion of the top 10 fatty acids in cultured meat (C) or pork (D) of C8-C22 fatty acids. Others: proportion of outside the top 10 fatty acids in cultured meat or pork of C8-C22 fatty acids.

acids between pork and cultured meat. Error bars indicate s.e.m, $n = 4$ of each group. *** $P < 0.01$, *** $P < 0.001$, *** $P < 0.0001$, ns: not significant. **C, D** Detailed Proportion of the top 10 fatty acids in cultured meat (C) or pork (D) of C8-C22 fatty acids. Others: proportion of outside the top 10 fatty acids in cultured meat or pork of C8-C22 fatty acids.

the template. Following the manufacturer's instructions, the CMV-pig *MyoD* fragment was ligated into the shuttle plasmid using homologous recombinase (Yugong Bio, EG21202s). The recombinant shuttle plasmid was then transformed into DH5 α competent cells (Angyu Bio, G6016-01), which were plated on LB solid medium and incubated overnight. Single colonies were selected and cultured in LB liquid medium for 6–8 h. The shuttle plasmid vector sequence was verified through Sanger sequencing. The plasmid was extracted using a plasmid extraction kit (Aidlab Bio, PL04).

Packaging of *MyoD* overexpressing adenovirus: The shuttle plasmid and adenovirus backbone plasmid were co-transfected into HEK-293A cells using jetPRIME (Polyplus, 101000046) at a ratio of 1:1 for 6 h. The cells were cultured in DMEM medium (Gibco, C11995500BT) containing 10% Fetal bovine serum (Wenren, 0801-WH) at 37 °C in a 5% CO₂ environment. Once approximately 50% of the cells had died, the cell suspension was collected, centrifuged at 1000 rpm for 5 min to collect the cell pellet, and subjected to five freeze-thaw cycles after adding 200 μ L of medium. The mixture was then centrifuged at 4000 rpm for 5 min, and the supernatant containing the first-generation adenovirus was collected. The virus supernatant was used to re-infect HEK-293A cells until the third-generation adenovirus was obtained, which was aliquoted and stored at -80 °C.

Preparation of olive oil-based lipogenic inducer

As an example for preparing 50 mL of olive oil-based lipogenic inducer: Aqueous phase: 1.1 g of glycerol was dissolved in 34 mL of PBS (Solarbio, P1020), and the solution was heated in a 70 °C water bath. Oil phase: 10 g of olive oil (Oilvoila) and 5 g of soybean lecithin (Solarbio, L8050) were weighed, and the mixture was stirred for 6 h at 70 °C under helium protection. The aqueous phase and oil phase were mixed and stirred at 60 °C for 3 h, then sheared at high speed at 10,000 rpm for 10 min, followed by ultrasonic shaking for 2 h. The pH was adjusted to 7.0–8.0 using 0.1 mol/L sodium hydroxide solution, and finally, the mixture was sterilized by autoclaving. The resulting olive oil-based lipogenic inducer had an olive oil concentration of 200 mg/mL.

3D cell culture and isolation

Porcine fibroblasts were isolated from 35-day Bama miniature pig embryos. The animal experiments were approved by Shandong Agricultural University Animal Care and Use Committee (SDAUA-2023-055). We have complied with all relevant ethical regulations for animal use. 3D cell culture: 0.6 g of GelMA-PEO (Engineering For Life, EFL-GM-PR-002) was dissolved in 10 mL of PBS, with 24 mg of lithium acylphosphinate salt photoinitiator (LAP) included in the GelMA. The mixture was stirred at 37 °C in

Table 1 | List of primers of qPCR

Gene	Forward primer	Reverse primer
MyoD	CTGCTACGACGGCACCTATT	CACGATGCTGGACAGACAG
MyoG	GCAGGCTCAAGAAGGTGAAT	GCACTCGATGTACTGGATGG
Myf5	CTCCGACGGCATGCCTGAAT	CCAGGCTGGATAAGGAGCTTT
Myf6	GATGACTGCGAAGGAAGGAGG	TCCGGCCGCGAGTTATTC
DGAT1	CGAGCTCAACTTTCCCGCT	GCTGGATGAGGAACAGCATCT
DGAT2	GTTCCCTGGCATAAAGCCCT	CAGACATCAGGTACTCCCCG
GAPDH	TCTTCTGGGTGGCAGTGAT	GTTTGTGATGGCGTGAA

the dark for 1 h to dissolve. It was then immediately filtered through a 0.22 µm filter to obtain a 6% w/v GelMA hydrogel solution, which was kept at 37 °C in the dark for later use or stored at -20 °C. The cells were treated with trypsin (Gibco, 25200072), then gently mixed with the GelMA hydrogel solution by pipetting. The mixture was transferred into a curing mold and allowed to stand for 30 s, then exposed to a 405 nm curing light source for 30–45 s. The cells were cultured in growth medium at 37 °C in a 5% CO₂ environment. Growth medium consists of 15% FBS, 1% penicillin and streptomycin (AA) and DMEM.

3D cell isolation: The cell-hydrogel complex was rinsed three times with PBS, then 1 mL of collagenase II enzyme (Solarbio, C8150) was added and the mixture was digested at 37 °C for 5 min. Afterward, the hydrogel was removed and broken into small pieces, then placed back at 37 °C for digestion until the cells became rounded and detached from the hydrogel. Culture medium was added to terminate digestion, and the mixture was centrifuged at 1000 rpm for 5 min to obtain a cell pellet.

EdU assay

The cell-hydrogel complex was incubated with a culture medium containing 1 µL/mL of 5-ethynyl-2'-deoxyuridine (EdU) for 6 h. Then, the cells were fixed using 4% paraformaldehyde (PFA) for 30 min. The cells were stained with the prepared staining solution for 6 h, which consisted of 1 mmol/L CuSO₄, 100 mmol/L Tris-HCl, 100 mmol/L ascorbic acid, and 1:1000 Alexa Fluor 555 Azide⁴⁹. Finally, the cells were stained with DAPI (Solarbio, C0060) for 15 min.

Scanning Electron Microscopy (SEM)

The scaffolds were plunged into liquid nitrogen and ruptured. Scaffolds were dried by supercritical drying and scanned using SEM (HITACHI Regulus 8100) to observe the microstructure of the scaffolds.

For SEM analysis of scaffolds seeded with cells, scaffolds were fixed with 2.5% glutaraldehyde for 24 h at 4 °C and dehydrated in ascending series of ethanol. Scaffolds were dried by supercritical drying and sputter-coated with gold and observed by SEM.

Cell viability and differentiation

To assess cell viability, cells were labeled with Calcein-AM (live cells in green, beyotime, C1367S) and propidium iodide (dead cells in red, beyotime, ST511). Briefly, cell medium was removed and replaced by a mixture of Calcein-AM and PI diluted in a culture medium solution. After 30 min incubation at 37 °C in a humidified atmosphere containing 5% CO₂, hydrogels were immediately examined under fluorescence microscopy and confocal microscopy (Andor Dragonfly 200).

For the myogenic transdifferentiation of porcine fibroblasts, after allowing the cells to grow for about 7 days to an appropriate density, a microinjection syringe was used to uniformly inject a suitable volume of adenoviral solution and polyethyleneimine into the hydrogel. After 48 h, the medium was replaced to myogenic differentiation medium for 7 days. Myogenic differentiation medium contains 2% horse serum (HS) (Procell, 164215), 1% AA, and DMEM.

For the formation of lipid droplets in porcine fibroblasts, after allowing the cells to grow for about 7 days to an appropriate density, lipogenic

medium was added and the cells were cultured for 2 days. Lipogenic medium contains an appropriate amount of olive oil-based lipogenic inducers (calculated based on the required concentration), 15% FBS, 1% AA, and DMEM.

For the co-induction of muscle and fat in porcine fibroblasts, myogenic transdifferentiation was first performed as described above. After culturing in myogenic differentiation for 5 days, the medium was replaced with myogenic and lipogenic medium for 2 days. Myogenic and lipogenic medium is a co-culture medium for muscle and fat that contains an appropriate amount of olive oil-based lipogenic inducer (calculated based on the required concentration), 2% HS, 1% AA, and DMEM.

Immunofluorescence staining

Similar to our previous steps for immunofluorescence staining of cells in 2D culture⁵⁰, due to the obstruction caused by the hydrogel, the staining time was extended. The cell-hydrogel complex was fixed in 4% PFA for 30 min and was washed three times with PBS. Then, it was permeabilized with PBS containing 0.5% Triton X-100 for 30 min. The complex was blocked with PBS containing 10% goat serum for 12 h at 4 °C. It was then incubated with MHC primary antibody (DSHB, AB2147781) for 24 h at a dilution of 1:100. Following that, it was incubated with Alexa secondary antibody (Solarbio, K0055G-AF555) for 6 h at a dilution of 1:500. The nucleus was stained with DAPI for 15 min and observed using fluorescence microscopy and confocal microscopy (Andor Dragonfly 200).

Oil Red O staining

The cell-hydrogel complex was fixed with 4% PFA for 30 min. The complex was infiltrated with 60% isopropanol for 30 min. Oil Red O (Sigma, #O0625) was used for staining for 60 min. The complex was washed three times with PBS, each time for 5 min. It was then washed with 60% isopropanol for 60 s to remove excess stain. Finally, it was rinsed with PBS for 5 min and observed under a microscope.

RNA extraction

After the cells were separated from the hydrogel, RNA was extracted using an RNA extraction kit (Tiangen, DP419). The RNA concentration was measured using a NanoDrop 2000 (Thermo Scientific, USA).

Quantitative Real-Time PCR

The extracted RNA was reverse transcribed into single-stranded cDNA using an RT reagent kit (Yugong Bio, EG15133S), with an RNA input amount of 500–800 ng. Real-time quantitative PCR was performed using SYBR Green Mix (Accurate Bio, A5A0923) following the manufacturer's instructions. Expression was normalized to GAPDH using delta-delta-CT method. For comparisons of the expression, we used a one-tailed Student's t-test. The error bars indicate the SEM. The RT-qPCR primers are described in Table 1.

Western Blotting

The cell pellet was collected, and a cell lysis buffer (Ncmbio, p70100) and protein lysis (Ncmbio, p001) were added at a volume ratio of 50:1. After lysing for 10 minutes, the mixture was centrifuged at 12,000 r/min for 5 min at 4 °C to obtain the protein supernatant. The proteins were denatured and

separated by electrophoresis on a 10% ExpressCast PAGE (Ncmbio, P2012), followed by transfer to a polyvinylidene fluoride (PVDF) membrane (Merck, ISEQ00010). The PVDF membrane was blocked in blocking buffer (Ncmbio, p30500) for 10 minutes and washed three times with TBST (Yugong Bio, CP17209M) for 10 min each. Then the PVDF membrane was incubated with MHC antibody diluted 1:1000 and GAPDH antibody (abclonal, AC027) diluted 1:1000 at 4 °C for 6 h, followed by three washes with TBST. Subsequently, the membrane was incubated with HRP Goat Anti-Mouse Anti-Rabbit IgG (abclonal, AS080) diluted 1:1000 at room temperature for 1 h and then washed with TBST. The visualization of blot signals on the PVDF membrane was performed using NcmECL Ultra (Ncmbio, P10100) on a C300 imaging system (Azure Biosystems, CA).

Western blot band intensities were quantified using ImageJ (1.8.0). The relative expression values (target protein/GAPDH) were used for statistical analysis.

Determination of fatty acid composition

Samples of cultured meat cells and pork hind leg muscle were taken, with four parallel samples set up for each group, and sent to Zhongke Zhidian Biotechnology Co., Ltd. for the determination of C₈ to C₂₂ fatty acid.

Statistics and Reproducibility

Statistical analyses were performed using the GraphPad Prism software. For comparisons between two independent groups, an unpaired two-tailed Student's t-test was used. For experiments involving comparisons across three independent groups, one-way analysis of variance (ANOVA) was applied. Post hoc multiple comparisons were conducted using Tukey's test to identify significant differences between time points. Measurements were obtained from independent biological replicates at each time point, with no repeated measurements on the same sample. All data are presented as mean ± standard deviation (SD). The sample size (n), statistical test used, and p-values are reported in the corresponding figure legends. The significance of differences is provided in the figure legends. Sample sizes ≥3. All key experiments were independently replicated at least three times with consistent results across replicates.

Material and data Availability

All newly generated plasmids in this study are available from the corresponding author upon request.

Reporting summary

Further information on research design is available in the Nature Portfolio Reporting Summary linked to this article.

Data availability

All data are included in this published article. Values for all data points can be found in Supplementary Data 1. Uncropped blots are provided in Supplementary Fig S6.

Received: 11 October 2024; Accepted: 22 July 2025;

Published online: 29 July 2025

References

1. Tuomisto, H. L. & de Mattos, M. J. Environmental impacts of cultured meat production. *Environ. Sci. Technol.* **45**, 6117–6123 (2011).
2. Mattick, C. S., Landis, A. E. & Allenby, B. R. A case for systemic environmental analysis of cultured meat. *J. Integr. Agriculture* **14**, 249–254 (2015).
3. Post, M. J. Cultured meat from stem cells: challenges and prospects. *Meat Sci.* **92**, 297–301 (2012).
4. Hadi, J. & Brightwell, G. Safety of alternative proteins: technological, environmental and regulatory aspects of cultured meat, plant-based meat, insect protein and single-cell protein. *Foods* **10**, 1226 (2021).
5. Balasubramanian, B., Liu, W., Pushparaj, K. & Park, S. The Epic of In Vitro Meat Production—A Fiction into Reality. *Foods* **10**, 1395 (2021).
6. Jin, G. & Bao, X. Tailoring the taste of cultured meat. *Elife* **13**, e98918 (2024).
7. Lee, M. et al. Cultured meat with enriched organoleptic properties by regulating cell differentiation. *Nat. Commun.* **15**, 77 (2024).
8. Chriki, S. & Hocquette, J. F. The myth of cultured meat: a review. *Front Nutr.* **7**, 7 (2020).
9. Hocquette, J. F., Chriki, S., Fournier, D. & Ellies-Oury, M. P. Review: Will “cultured meat” transform our food system towards more sustainability?. *Animal* **19**, 101145 (2025).
10. Lee, S. Y. et al. Current technology and industrialization status of cell-cultivated meat. *J. Anim. Sci. Technol.* **66**, 1–30 (2024).
11. Fraeye, I., Kratka, M., Vandeburgh, H. & Thorrez, L. Sensorial and nutritional aspects of cultured meat in comparison to traditional meat: much to be inferred. *Front Nutr.* **7**, 35 (2020).
12. Zhu, H. et al. Production of cultured meat from pig muscle stem cells. *Biomaterials* **287**, 121650 (2022).
13. Zhu, G. et al. Generation of three-dimensional meat-like tissue from stable pig epiblast stem cells. *Nat. Commun.* **14**, 8163 (2023).
14. Liu, P. et al. Preparation and quality evaluation of cultured fat. *J. Agric Food Chem.* **71**, 4113–4122 (2023).
15. Hauser, M., Zirman, A., Rak, R. & Nachman, I. Challenges and opportunities in cell expansion for cultivated meat. *Front Nutr.* **11**, 1315555 (2024).
16. Kim, D. H., Lee, J., Suh, Y., Cressman, M. & Lee, K. Research Note: Adipogenic differentiation of embryonic fibroblasts of chicken, turkey, duck, and quail in vitro by medium containing chicken serum alone. *Poult. Sci.* **100**, 101277 (2021).
17. Yin, J. et al. In vitro myogenic and adipogenic differentiation model of genetically engineered bovine embryonic fibroblast cell lines. *Biotechnol. Lett.* **32**, 195–202 (2009).
18. Fernandes, I. R. et al. Fibroblast sources: where can we get them?. *Cytotechnology* **68**, 223–228 (2016).
19. Pasitka, L. et al. Spontaneous immortalization of chicken fibroblasts generates stable, high-yield cell lines for serum-free production of cultured meat. *Nat. Food* **4**, 35–50 (2023).
20. Jeong, D. et al. Efficient myogenic/adipogenic transdifferentiation of bovine fibroblasts in a 3D bioprinting system for steak-type cultured meat production. *Adv. Sci. (Weinh.)* **9**, e2202877 (2022).
21. Ren, R. et al. Characterization and perturbation of CTCF-mediated chromatin interactions for enhancing myogenic transdifferentiation. *Cell Rep.* **40**, 111206 (2022).
22. Wardle, F. C. Master control: transcriptional regulation of mammalian Myod. *J. Muscle Res. Cell Motil.* **40**, 211–226 (2019).
23. Rudnicki, M. A. et al. MyoD or Myf-5 is required for the formation of skeletal muscle. *Cell* **75**, 1351–1359 (1993).
24. Kassar-Duchossoy, L. et al. Mrf4 determines skeletal muscle identity in Myf5:Myod double-mutant mice. *Nature* **431**, 466–471 (2004).
25. Chan, S. S. & Kyba, M. What is a master regulator? *J. Stem Cell Res. Ther.* **3**, 114 (2013).
26. Nabeshima, Y. et al. Myogenin gene disruption results in perinatal lethality because of severe muscle defect. *Nature* **364**, 532–535 (1993).
27. Hasty, P. et al. Muscle deficiency and neonatal death in mice with a targeted mutation in the myogenin gene. *Nature* **364**, 501–506 (1993).
28. Ma, T. et al. Transdifferentiation of fibroblasts into muscle cells to constitute cultured meat with tunable intramuscular fat deposition. *Elife* **13**, RP93220 (2024).
29. Li, X., Fu, X., Yang, G. & Du, M. Review: enhancing intramuscular fat development via targeting fibro-adipogenic progenitor cells in meat animals. *Animal* **14**, 312–321 (2020).
30. Lucher, L. W. et al. Consumer and trained panel evaluation of beef strip steaks of varying marbling and enhancement levels cooked to three degrees of doneness. *Meat Sci.* **122**, 145–154 (2016).
31. Louis, F., Furuhashi, M., Yoshinuma, H., Takeuchi, S. & Matsusaki, M. Mimicking Wagyu beef fat in cultured meat: Progress in edible bovine

adipose tissue production with controllable fatty acid composition. *Mater. Today Bio* **21**, 100720 (2023).

32. Yanting, C. et al. Dose- and type-dependent effects of long-chain fatty acids on adipogenesis and lipogenesis of bovine adipocytes. *J. Dairy Sci.* **101**, 1601–1615 (2018).

33. Scott, M. A., Nguyen, V. T., Levi, B. & James, A. W. Current methods of adipogenic differentiation of mesenchymal stem cells. *Stem Cells Dev.* **20**, 1793–1804 (2011).

34. Mehta, F., Theunissen, R. & Post, M. J. Adipogenesis from bovine precursors. *Methods Mol. Biol.* **1889**, 111–125 (2019).

35. Marcelino, G. et al. Effects of olive oil and its minor components on cardiovascular diseases, inflammation, and gut microbiota. *Nutrients* **11**, 1826 (2019).

36. Ying, G. L. et al. Aqueous two-phase emulsion bioink-enabled 3D Bioprinting of Porous Hydrogels. *Adv. Mater.* **30**, e1805460 (2018).

37. Rubio, N. R., Xiang, N. & Kaplan, D. L. Plant-based and cell-based approaches to meat production. *Nat. Commun.* **11**, 6276 (2020).

38. Sinke, P., Swartz, E., Sanctorum, H., van der Giesen, C. & Odegard, I. Ex-ante life cycle assessment of commercial-scale cultivated meat production in 2030. *Int. J. Life Cycle Assess.* **28**, 234–254 (2023).

39. Petersen, K. S. et al. Perspective on the health effects of unsaturated fatty acids and commonly consumed plant oils high in unsaturated fat - CORRIGENDUM. *Br. J. Nutr.* **132**, 1051 (2024).

40. Rajaram, S. Health benefits of plant-derived α -linolenic acid. *Am. J. Clin. Nutr.* **100**, 443S–448S (2014).

41. Mancini, A. et al. Biological and nutritional properties of palm oil and palmitic acid: effects on health. *Molecules* **20**, 17339–17361 (2015).

42. Kaur, N., Chugh, V. & Gupta, A. K. Essential fatty acids as functional components of foods- a review. *J. Food Sci. Technol.* **51**, 2289–2303 (2014).

43. Guo, X. et al. The relationship between lipid phytochemicals, obesity and its related chronic diseases. *Food Funct.* **9**, 6048–6062 (2018).

44. Basak, S. & Duttaroy, A. K. Conjugated linoleic acid and its beneficial effects in obesity, cardiovascular disease, and cancer. *Nutrients* **12**, 1913 (2020).

45. Santamarina, A. B. et al. Anti-inflammatory effects of oleic acid and the anthocyanin keracyanin alone and in combination: effects on monocyte and macrophage responses and the NF- κ B pathway. *Food Funct.* **12**, 7909–7922 (2021).

46. Yuen, J. S. K. Jr. et al. Aggregating in vitro-grown adipocytes to produce macroscale cell-cultured fat tissue with tunable lipid compositions for food applications. *Elife* **12**, e82120 (2023).

47. Mitic, R., Cantoni, F., Berlin, C. S., Post, M. J. & Jackisch, L. A simplified and defined serum-free medium for cultivating fat across species. *iScience* **26**, 105822 (2023).

48. Lee, M. et al. Flavor-switchable scaffold for cultured meat with enhanced aromatic properties. *Nat. Commun.* **15**, 5450 (2024).

49. Zhang, H. et al. Disturbance of calcium homeostasis and myogenesis caused by TET2 deletion in muscle stem cells. *Cell Death Discov.* **8**, 236 (2022).

50. Luo, W. et al. Retinoic acid and RAR γ maintain satellite cell quiescence through regulation of translation initiation. *Cell Death Dis.* **13**, 838 (2022).

(ZR2024MC096), Postdoctoral Fellowship Program of CPSF (ZC20231499), Taishan Scholar Program (202211100), Scientific Research Innovation Team of Young Scholar of Shandong.

Author contributions

P.Z., J.L. performed the experiments and collected data. W.G., H.M., H.C., L.C. and A.K. contributed to the analysis of cell viability and lipid profile. J.L., P.Z. and H.W. wrote the article. All authors edited the manuscript.

Ethics declarations

The animal experiments were approved by Shandong Agricultural University Animal Care and Use Committee (SDAUA-2023-055). We have complied with all relevant ethical regulations for animal use.

Competing interests

The authors declare no competing interests.

Additional information

Supplementary information The online version contains supplementary material available at <https://doi.org/10.1038/s42003-025-08574-y>.

Correspondence and requests for materials should be addressed to Heng Wang.

Peer review information *Communications Biology* thanks Min Du, Martin Rasmussen, and the other, anonymous, reviewer for their contribution to the peer review of this work. Primary Handling Editor: Christina Karlsson Rosenthal.

Reprints and permissions information is available at <http://www.nature.com/reprints>

Publisher's note Springer Nature remains neutral with regard to jurisdictional claims in published maps and institutional affiliations.

Open Access This article is licensed under a Creative Commons Attribution-NonCommercial-NoDerivatives 4.0 International License, which permits any non-commercial use, sharing, distribution and reproduction in any medium or format, as long as you give appropriate credit to the original author(s) and the source, provide a link to the Creative Commons licence, and indicate if you modified the licensed material. You do not have permission under this licence to share adapted material derived from this article or parts of it. The images or other third party material in this article are included in the article's Creative Commons licence, unless indicated otherwise in a credit line to the material. If material is not included in the article's Creative Commons licence and your intended use is not permitted by statutory regulation or exceeds the permitted use, you will need to obtain permission directly from the copyright holder. To view a copy of this licence, visit <http://creativecommons.org/licenses/by-nc-nd/4.0/>.

© The Author(s) 2025

Acknowledgements

This work was supported by the National Science Foundation of China (31771617), Shandong Provincial Natural Science Foundation